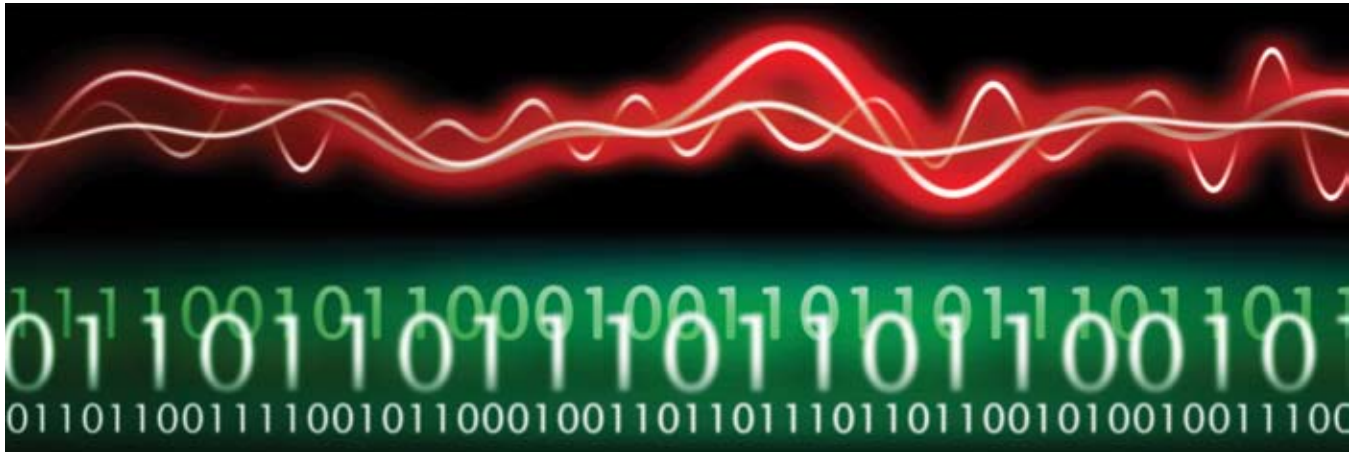


Local Oscillator Phase Noise Effects on GNSS Code Tracking



© iStockphoto.com/Eugene Kazimiravitch

A new perspective for GNSS designers quantifies the performance loss due to phase noise effects on the baseband signal. These performance bounds may then be used as the basis for local oscillator design. The authors develop bounds by identifying front-end local oscillator phase noise effects on the correlation loss, while tracking receiver performance. Until now, this effect has been rarely documented in research literature. Extensive simulations are used to validate results, while drawing conclusions regarding the relationship between phase noise, correlation time, and loss in the carrier-to-noise ratio.

GPS | GALILEO | GLONASS | COMPASS

ERNESTO PÉREZ SERNA,
ACORDE TECHNOLOGIES S.A

SARANG THOMBRE, MIKKO VALKAMA, SIMONA LOHAN, VILLE SYRJÄLÄ
TAMPERE UNIVERSITY OF TECHNOLOGY

MARCO DETRATTI
ACORDE TECHNOLOGIES S.A

HEIKKI HURSKAINEN, JARI NURMI
TAMPERE UNIVERSITY OF TECHNOLOGY

GNSS systems rely on direct sequence spread spectrum (DSSS) transmissions to achieve high receiver sensitivity. Typically, GNSS user equipment compares the signal received from a satellite with an internally generated replica of its corresponding code until the maximum

correlation for a given delay is achieved. This provides an indirect measurement of the satellite-receiver range.

One of the performance limiting factors of GNSS receivers is the imperfection of the radio frequency (RF) oscillator. This imperfection translates into random deviations of instantaneous phase or frequency, typically modeled as a phase imperfection, and often referred to as phase noise.

The receiver oscillator phase noise narrows the carrier tracking loop bandwidth, while diminishing the achievable carrier-to-noise ratio (C/N_0). The correlation outputs in the code-tracking loop are also affected, creating correlation noise and losses at the receiver that are measured as reductions in C/N_0 .

Furthermore, longer integration intervals ideally result in higher sensitivity. However, because phase noise is translated into a rotation of the constellation diagram of a modulated signal that can make integration (correlation) comparatively less effective as the interval increases.

Phase noise models have been proposed for various wireless communication receivers. (See the sidebar, “Modeling Phase Noise Effects on Receivers: A History” on [page 54](#).) However, the effects of phase noise on GNSS receivers’ performance have been rarely documented, leaving key design questions unanswered: *What is the maximum acceptable phase noise level as required by an RF designer in order to achieve a*

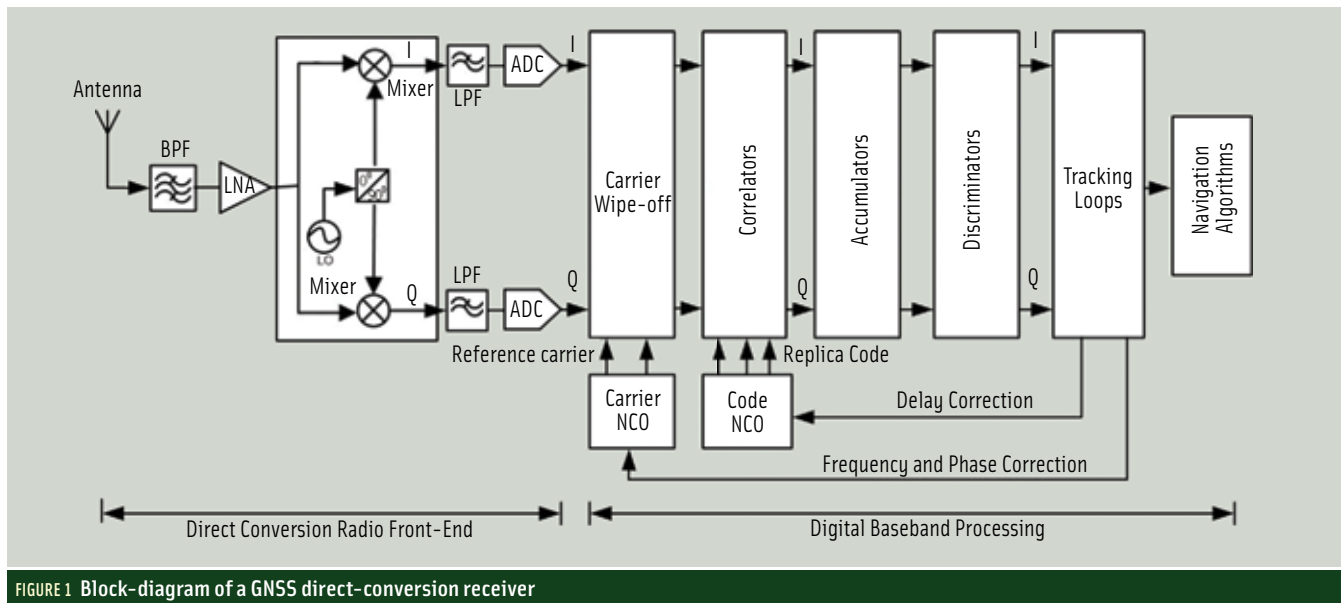


FIGURE 1 Block diagram of a GNSS direct-conversion receiver

minimum pre-defined C/N_0 ? How do correlation losses relate to phase noise levels?

In this article, we propose an analytical approach using a given phase noise model, validating it through simulations to quantify the effect of oscillator noise on the performance of GNSS receivers. From this we provide a first estimation of the requirements of a radio front-end for a given baseband implementation, as well as an insight into the relationship between correlation time and performance degradation due to phase noise. The following section of our discussion provides a theoretical analysis, in both time-domain and frequency-domain, of the effect of this phase noise on various properties of code correlation.

We then perform numerical simulations of GPS L1 pseudorandom noise (PRN) code correlation for various values of phase noise in order to validate the theoretical model. Next, a datastream simulation using a Galileo E1 receiver, complete with carrier and code tracking loops, quantifies the effect of oscillator noise on GNSS receiver performance. Here, the simulated PRN code correlation in the presence of phase noise demonstrates that the model (and GPS results) may be applied to Galileo signal receivers as well.

Finally, we compare results from all the simulations and recommend a practical limit for the maximum phase noise permissible from the front-end oscillator in order to maintain the post-correlation signal-to-noise ratio (SNR) of a correlation peak beneath a given threshold.

Our results provide a first estimate of the noise floor requirements for a receiver given a particular baseband implementation. Also, this study provides insight into the relationship between correlation time and performance degradation due to phase noise.

Phase Noise Model

Figure 1 shows the block diagram of a typical GNSS receiver

considered for this study. Let us first consider the operation of the local oscillator (LO) in a receiver.

Any oscillator is defined by three parameters: phase (φ), amplitude (A), and frequency (f_0). In a general case phase and amplitude noise exist, as well as distortion, which makes both A and φ functions of time, such that

$$w(t) = A(t) \cos(2\pi f_0 t + \varphi(t)) \quad (1)$$

The nonlinear dynamics of an oscillator make the amplitude $A(t)$ relatively constant, so it becomes considerably less important than phase noise. Furthermore, if the modulation used to carry information does not affect the amplitude, the receiver can also ignore this component. Phase noise, however, cannot be overlooked, and it actually becomes the defining parameter of the quality of any oscillator.

Phase noise specifications are typically given in decibels relative to the carrier per hertz (dBc/Hz) at a certain frequency offset, f_m , from the desired center frequency of the oscillator. Phase noise $\Phi(t)$ for a free running oscillator is a non-stationary random variable, and $e^{j\Phi(t)}$ is a stationary random variable whose power spectral density (PSD), $P_x(f)$, is given in Equation 2.

$$P_x(f) = \begin{cases} \frac{\sigma_\Phi^2}{(2\pi f)^2 + (\frac{\sigma_\Phi^2}{2})^2} & \sigma_\Phi^2 \neq 0 \\ \delta(f) & \sigma_\Phi^2 = 0 \end{cases} \quad (2)$$

where σ_Φ^2 is the unit time variance of the random phase noise process, so that total variance is measured by $\sigma_\Phi^2(t)$. In terms of PSD, the phase noise is given by:

$$L(f_m) = 10 \log_{10}(P_x(f_m))$$

where $L(f_m)$ is the phase noise in units of dBc/Hz, and $P_x(f_m)$ is given by simplifying Equation 2 as shown in Equation 3:

$$P_x(f) = \frac{\sigma_\phi^2}{(2\pi f_m)^2 + (\frac{\sigma_\phi^2}{2})^2} \approx \frac{\sigma_\phi^2}{(2\pi f_m)^2} \quad \text{if } \frac{\sigma_\phi^2}{(f_m)^2} \text{ is small} \quad (3)$$

and further simplifying phase noise to:

$$L(f_m) \approx 20 \log \left(\frac{\sigma_\phi}{2\pi f_m} \right) \text{ dBc/Hz} \quad (4)$$

where f_0 is the oscillation frequency, f_m is the frequency offset, and σ_ϕ is the constant that defines the noise level of the oscillator. In practice all free-running oscillators show a noise roll-off of 20 decibels per decade when far enough from the fundamental frequency.

The defining assumption of this model is that the phase difference between time instants t_1 and t_2 follows a Gaussian distribution with null mean and variance linearly increasing with the length of the interval, also known as Wiener or random-walk processes, thus

$$E \left[(\varphi(t_2) - \varphi(t_1))^2 \right] = \sigma_\phi^2 |t_2 - t_1| \quad (5)$$

This model is also suitable for PLL-based synthesizers with narrow loop bandwidths where the voltage controlled oscillator (VCO) noise dominates. Even though there are significant differ-

Modeling Phase Noise Effects on Receivers: A History

In 1966 D.B. Leeson proposed an empirical linear model for the noise spectrum of an oscillator, which has been extensively cited in the literature since then. G. Sauvage generalized this model to other resonant circuits in 1977, providing a deeper mathematical background. In 1998 A. Hajimiri and T.H. Lee proposed a linear time variant model (LTV) to explain the effect of each of the noise sources of an oscillator on its phase noise.

Phase noise models for various wireless communication receivers have been proposed by T. Schenk (2006) (For the complete citations of this and other references, please see the Additional Resources section near the end of the main article.) The article by D. Petrovic *et alia* uses orthogonal frequency division multiplexing (OFDM) systems for modeling noise, while A. Demir *et alia* (2000) developed extensive and generic theory for phase noise models. In a 2002 article, Demir extended this theory to jitter in optical and wireless communications, and K. Kundert also developed a jitter measurement for phase noise effects on phase locked loops.

A simulation-based study of phase noise introduced by the receiver and the satellite payload was discussed by E. Rebeyrol *et alia* in 2006. Deriving the phase noise power spectral densities, frequency comparisons are made, but correlation losses or effects on the code tracking loop at the receiver were not included. M. Irsigler and B. Eissfeller discuss the impact of oscillator phase noise on the performance of the PLL tracking in their 2002 article, while modeling theoretical results, but they draw no conclusions regarding the phase noise requirements of the oscillator. Their analysis focused on classification of the phase noise sources and types and on the phase lock loop tracking performance at fixed phase noise random vibrations and Allan deviations.

In 2010, M. Petovello *et alia* discuss the effect of residual phase noise in the carrier tracking loop on the performance of C/N_0 estimation algorithms, but do not identify the effect on the code tracking loop. A. Demir *et alia* (2006) provides a thorough analysis of the spectral characteristics of phase noise. In 2010 Schenk demonstrated that is a stationary random variable defined for a free running local oscillator whose power spectral density (PSD), $P_x(f)$, as given in Equation 2 in the main article.

ences in the results when other phase noise models are considered, this can still be considered a first approach to the problem.

Phase Noise and Code Correlation

Let us turn now to the factors involved in the effects of phase noise on code correction.

Post-Correlation Signal to Noise Ratio. Letting $x(t)$ be an ideal real signal, having no quadrature component, we initially modulate a carrier at ω_0 as $x(t) \cdot e^{j\omega_0 t}$. Complex down-conversion, assuming coherent detection, is described by (6):

$$y(t) = y_I(t) + jy_Q(t) = x(t)e^{j\omega_0 t} e^{-j\omega_0 t} = x(t) \quad (6)$$

where the down-converted signal is then correlated with an aligned replica over a period T . If the code is optimally aligned, Equation 7 results:

$$|Y| = |I + jQ| = \left| \frac{1}{T} \int y_I(t)x(t)dt + j \frac{1}{T} \int y_Q(t)x(t)dt \right| \quad (7)$$

$$= \frac{1}{T} \left| \int x(t)x(t)dt \right|$$

Making several simplifications in the notation, we first normalize the energy of $x(t)$ over T (indicated as $|Y|$) to 1. Secondly, we assume that $x(t)$ equals $\{-1,1\}$, which is true for simple modulations such as binary phase shift keying (BPSK) or binary offset carrier (BOC(m,n)). Finally, we only consider pilot signals, excluding the factor of navigation data. Therefore, in the absence of phase noise,

$$|Y| = \frac{1}{T} \left| \int 1dt \right| = 1 \quad (8)$$

Let us now consider the effect of the phase noise of the local oscillator where the carrier is down-converted with an additional random phase $\varphi(t)$, thus:

$$y(t) = y_I(t) + jy_Q(t) = x(t)e^{j\omega_0 t} e^{-j\omega_0 t + j\varphi(t)} \quad (9)$$

$$= x(t)e^{j\varphi(t)}$$

$$|Y| = |I + jQ| = \left| \frac{1}{T} \int_0^T \cos\varphi(t)dt + j \frac{1}{T} \int_0^T \sin\varphi(t)dt \right| \quad (10)$$

During the correlation process in a GNSS receiver, this signal is multiplied by an ideal version of itself. Theoretically, when both are perfectly aligned the integral or area of the resulting function is maximized. Calculating the correlation over a period containing phase variations or even inversions results in an energy *decrease*, because part of the signal is subtracted rather than added (or the other way around should the correlation be negative).

In general, phase noise has two effects on the signal. First, the signal may lose energy as the expected value of $|Y|$ decreases with noise, as described in Equation 11. Secondly, the variance of $|Y|$ — ideally 0 — increases, as shown in Equation 12.

$$E[|Y|] = E \left[\sqrt{I^2 + Q^2} \right] \equiv \mu_Y \leq 1 \quad (11)$$

$$\text{var}[|Y|] = E[|Y|^2] - E[|Y|]^2 \equiv \sigma_Y^2 \geq 0 \quad (12)$$

where μ_Y equals the mean or expected value of $|Y|$ and σ_Y^2 equals the variance of $|Y|$.

We can define the post-correlation SNR due to phase noise as the quotient of the square of the mean value of the autocorrelation peak and its variance:

$$SNR_{PN} \equiv 20 \log_{10} \left(\frac{\mu_Y}{\sigma_Y} \right) \quad (13)$$

As the accumulated phase shifts for a given noise level increase, the correlation time also increases. Thus, the integrated energy no longer increases linearly with time above certain phase noise levels, and eventually a point may be reached at which phase noise becomes dominant over post-correlation thermal noise, limiting the sensitivity increase one can obtain by increasing the correlation time. We present an explanation of this condition in the following section.

Mean Value of Correlation Peak. The average magnitude of the correlator output is calculated in order to estimate the noise and losses in the presence of phase noise. Instead of evaluating $E[|Y|]$ we will address $E[|Y|^2]$ which provides a similar metric while still allowing an analytical approach. Because noise is assumed to be low, where μ_Y is close to 1, we can easily see that

$$\mu_Y = E[|Y|] \approx \frac{1 + E[|Y|^2]}{2} \quad (14)$$

In the following paragraphs, we derive the relation between front-end oscillator phase noise and peak value of code correlation, using theoretical and analytical means in the time and frequency domains, respectively.

First, in the *time domain*, from Equation 11 we have,

$$E[|Y|^2] = E[I^2] + E[Q^2] \quad (15)$$

$$E[|Y|^2] = E \left[\left(\frac{1}{T} \int_0^T \cos \varphi(t) dt \right)^2 \right] E \left[\left(\frac{1}{T} \int_0^T \sin \varphi(t) dt \right)^2 \right]$$

$$\begin{aligned} E[I^2] &= \frac{1}{T^2} E \left[\int_0^T \cos \varphi(t_1) dt_1 \int_0^T \cos \varphi(t_2) dt_2 \right] \\ &= \frac{1}{T^2} E \left[\int_0^T \int_0^T \cos \varphi(t_1) dt_1 \cos \varphi(t_2) dt_2 \right] \\ &= \frac{1}{T^2} \int_0^T \int_0^T E[\cos \varphi(t_1) \cos \varphi(t_2)] dt_1 dt_2 \end{aligned} \quad (16)$$

We define the probability density function of the phase as

$$N(x, t) \equiv \frac{1}{\sqrt{2\pi} \sigma_\Phi \sqrt{t}} e^{-\frac{x^2}{2t\sigma_\Phi^2}}$$

If $t_2 > t_1$, then

$$\begin{aligned} E[\cos \varphi(t_1) \cos \varphi(t_2)] &= \iint \cos(a) N(a, t_1) \cos(a+b) N(b, t_2 - t_1) db da \\ &= \iint \cos(a) N(a, t_1) (\cos(a) \cos(b) - \sin(a) \sin(b)) N(b, t_2 - t_1) db da \end{aligned}$$

and due to odd symmetry:

$$\begin{aligned} E[\cos \varphi(t_1) \cos \varphi(t_2)] &= \iint \cos^2(a) N(a, t_1) \cos(a) N(b, t_2 - t_1) db da \\ &= \frac{1}{2} e^{-\frac{(t_2 - t_1)\sigma_\Phi^2}{2}} (1 + e^{-2t_1\sigma_\Phi^2}) \equiv f(t_1, t_2) \end{aligned}$$

Conversely, if $t_1 > t_2$, then:

$$\begin{aligned} E[\cos \varphi(t_1) \cos \varphi(t_2)] &= \frac{1}{2} e^{-\frac{(t_1 - t_2)\sigma_\Phi^2}{2}} (1 + e^{-2t_2\sigma_\Phi^2}) \equiv f(t_2, t_1) \\ E[I^2] &= \frac{1}{T^2} \int_{t_1=0}^T \int_{t_2=0}^{t_1} f(t_2, t_1) dt_2 dt_1 + \frac{1}{T^2} \int_{t_1=0}^T \int_{t_2=t_1}^T f(t_1, t_2) dt_2 dt_1 \end{aligned} \quad (17)$$

$$E[I^2] = \frac{1}{3} \frac{e^{-2T\sigma_\Phi^2} + 6T\sigma_\Phi^2 - 9 + 8e^{-\frac{T\sigma_\Phi^2}{2}}}{T^2\sigma_\Phi^4}$$

Following a similar approach it can be seen that

$$E[Q^2] = \frac{1}{3} \frac{e^{-2T\sigma_\Phi^2} + 6T\sigma_\Phi^2 - 15 + 16e^{-\frac{T\sigma_\Phi^2}{2}}}{T^2\sigma_\Phi^4} \quad (18)$$

and, therefore,

$$E[I^2 + Q^2] = \frac{4T\sigma_\Phi^2 + 8 \left(e^{-\frac{T\sigma_\Phi^2}{2}} - 1 \right)}{T^2\sigma_\Phi^4} \quad (19)$$

These losses due to noise are a function of $T\sigma_\Phi^2$, which is the phase noise variance over one code epoch (σ_Φ^2 is the rate at which the variance of the oscillator phase increases with time; so, $T\sigma_\Phi^2$ happens to be the phase variance at $t=T$). This follows intuitively because the variance of the phase increases linearly with time, which means scaling this phase noise has the same effect as applying this factor to the correlation time. For small values of $T\sigma_\Phi^2$ the following approximation can be made:

$$E[I^2 + Q^2] \approx 1 - \frac{T\sigma_\Phi^2}{6} \quad (20)$$

$$E[\sqrt{I^2 + Q^2}] \approx 1 - \frac{T\sigma_\Phi^2}{12} \quad (21)$$

In the *frequency domain* we can derive a theoretical expression for correlation losses using a free-running oscillator model in the RF front-end PLL. We assume that the PRN code is $c(t)$. For the sake of simplicity, we also assume that noise and multipath effects are absent.

The complex PRN code correlation output $R(\tau)$ at the receiver is obtained by correlating the incoming down-converted signal with a local reference code delayed by τ seconds. If we take into account the phase noise of the local oscillator, the correlation output can be written as:

$$R(\tau) = \int_0^T c(t) e^{j\Phi(t)} * c^*(t - \tau) dt \quad (22)$$

where

$e^{j\Phi(t)}$ = time-dependent phase noise effect,

$c^*(t-\tau)$ = time-delayed local code,

$\Phi(t)$ = non-stationary random variable modeling the phase noise effect, and

T = pre-detection integration time (PIT) over which code correlation is performed. (Note that T and PIT are the same, except that T is used in mathematical formulations and PIT in theoretical explanations; so, they should be mutually interchangeable.)

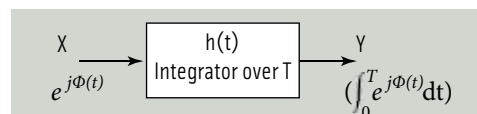


FIGURE 2 Equivalent model of phase noise effect.

The correlation peak has maximum value at $R(0)$ when the time delay between the incoming signal and the local replica is zero, in other words, when the two signals are perfectly aligned in time domain, as expressed by Equation 23:

$$\begin{aligned}
 R(0) &= R(\tau = 0) = \int_0^T c(t)e^{j\Phi(t)} * c^*(t) dt \\
 &= \int_0^T |c(t)|^2 e^{j\Phi(t)} dt \\
 &= \int_0^T e^{j\Phi(t)} dt
 \end{aligned}
 \tag{23}$$

We have considered $|c(t)|^2$ equals 1 because the PRN code $c(t)$ is essentially a binary sequence of +1s and -1s. Equation 23 shows that the correlation peak fluctuates randomly, according to $\Phi(t)$, and also shows that the effect of correlation peak in the presence of noise can be modeled as a filtered random variable $X = e^{j\Phi(t)}$ passed through an integrator filter, as shown in Figure 2.

The integrator impulse response is a rectangular pulse of width T:

$$h(t) = \begin{cases} 1 & 0 \leq t \leq T \\ 0 & \text{Otherwise} \end{cases}
 \tag{24}$$

Therefore, its frequency response is given by the well-known sinc function:

$$H(f) = T \frac{\text{Sin}(\pi f T)}{\pi f T}
 \tag{25}$$

The PSD of the input X from Figure 2 is given in Equation 2. Because X is a stationary random variable and $h(t)$ is linear filter, the PSD of the output random process Y (which corresponds to the fluctuations of the correlation peak $R(0)$) is given by Equation 26):

$$P_Y(f) = P_X(f) |H(f)|^2
 \tag{26}$$

The average power of the correlation peak is $E(R_2(0))$ equals $E(Y^2)$ and will be therefore calculated by integrating the PSD of Y over the whole frequency axis, as shown in equations 27 and 28:

$$\begin{aligned}
 E(R^2(0)) &= \int_{-\infty}^{\infty} P_X(f) |H(f)|^2 df \\
 \begin{cases} = T^2 \int_{-\infty}^{\infty} \frac{\sigma_\Phi^2}{(2\pi f)^2 + (\frac{\sigma_\Phi^2}{2})^2} \left[\frac{\text{Sin}(\pi f T)}{\pi f T} \right]^2 df & \text{for } \sigma_\Phi^2 \neq 0 \\ = T^2 & \text{for } \sigma_\Phi^2 = 0 \end{cases}
 \end{aligned}
 \tag{27}$$

where σ_Φ^2 equals 0 indicates absence of phase noise. The integral in Equation 27 for σ_Φ^2 not equal to 0 has been evaluated and its closed form expression is given by Equation 29:

$$E(R^2(0)) = \frac{-8+4T \sigma_\Phi^2 + 8e^{-\frac{T \sigma_\Phi^2}{2}}}{(\sigma_\Phi^2)^2} \quad \text{for } \sigma_\Phi^2 \neq 0
 \tag{29}$$

The mean value of correlation peak in presence of phase noise is therefore obtained by dividing Equation 29 by Equation 28:

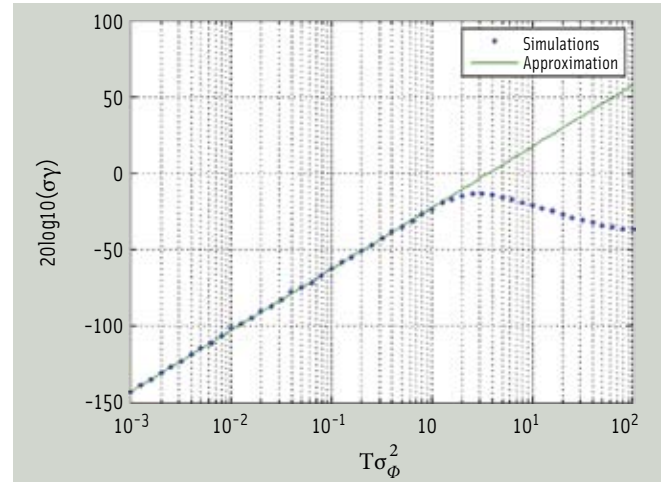


FIGURE 3 Variance of correlation peak.

$$E[I^2 + Q^2] = \frac{-8+4T \sigma_\Phi^2 + 8e^{-\frac{T \sigma_\Phi^2}{2}}}{T^2 (\sigma_\Phi^2)^2}
 \tag{30}$$

The loss or deterioration in correlation peak due to phase noise will be the inverse of Equation 30. This is, as expected, exactly the same result as that obtained by using the time domain analysis.

Correlation Noise. Signal losses due to phase variations during correlation already give the lower boundary for the phase noise specification. But this lower boundary alone does not represent the actual degradation of system performance.

It is reasonable to expect strong variations in the constellation (correlation noise) before the loss due to phase noise outweighs losses due to other factors in the receiver chain. The variance of the correlation peak, described by Equation 31, must be studied as well.

$$\sigma_Y^2 = \mu_Y^2 - E[|Y|^2]
 \tag{31}$$

Unfortunately, even though the first order approximation, given in Equation 14, is accurate enough to estimate losses, it is not a valid for obtaining σ_Y . However, because no analytical expression has been found for μ_Y , numerical approximations have been made in order to estimate σ_Y .

In the presence of relatively low noise levels, σ_Y increases linearly with $T\sigma_\Phi^2$. Adjusting the scale factor through simulations and defining the noise power (PN) logarithmically as PN equals $20 \log_{10}(\sigma_Y)$, we obtain the variance of the correlation peak:

$$PN_{\text{variance}} \text{ (dB)} \approx -22.6\text{dB} + 20\log_{10}(T\sigma_\Phi^2)
 \tag{32}$$

SNR_{PN} can now be estimated as long as noise is low enough for this first-order approximation to remain valid. Figure 3 shows that this approximation is appropriate where $T\sigma_\Phi^2$ less than 1.

Model for Correlation Between Phase Noise and Pure PRN Codes

In the previous section describing the effect of phase noise on code correlation, we derived a relation between front-end oscillator phase noise and peak value of code correlation in the time

and frequency domains, respectively. The next step is to prove this relation using a software-generated, simulation-based model of the code correlation process.

For this purpose, a numerical simulation program performed correlation between two versions of the same GPS PRN code. The first version was contaminated with various amounts of phase noise in order to replicate a real world PRN code received from the RF front-end and after the carrier strip-off process. The other version of the PRN code was kept ‘pure’ to mimic the local replica code as generated in every GNSS receiver. The model is diagrammatically represented in **Figure 4**.

The simulation software enables a user to select the satellite vehicle number whose PRN code is to be generated. In this case, we defined the phase noise in terms of unit time variance (σ_ϕ^2), which has units of radian² per second (Rad²/s). Therefore, the total phase noise variance per chip of the PRN code over the coherent integration period is given by Equation 33:

$$PN_{Variance} = \frac{T\sigma_\phi^2}{L_{PRN}} \quad (33)$$

where L_{PRN} is the length of the PRN code.

With the software, multiplication of the phase noise with incoming PRN code can be simulated as a multiplication of phase noise vector and PRN code vector. A random number “noise” vector with zero mean, unity standard deviation, and length of 1,023 bits was created. Its variance was changed to the required phase noise variance using the $PN_{variance}$ calculated in Equation 33.

The model for phase noise of a free-running oscillator is of the form where the instantaneous phase value is a cumulative sum of uncorrelated Gaussian random variables over the whole past history — in other words, the integral of white Gaussian noise.

Integrating over wider and wider time windows creates a process with a linearly increasing variance over time, and, thus, it is non-stationary. However, because the complex exponential of the phase noise ($e^{j\Phi(t)}$) is a stationary random variable, it can be used instead of just phase noise ($\Phi(t)$).

Having achieved a phase noise vector of the desired length and noise variance, we can now multiply it by a PRN code vector in order to produce a noisy PRN code similar to the one obtained from the RF front-end in a real-world GNSS receiver.

Correlation of this noisy code is performed with a “pure” PRN code over multiple iterations. Once we have all iterations for one value of phase noise variance are complete, we then may calculate the mean of the correlation peak for the present value of σ_ϕ^2 . Varying σ_ϕ^2 from 0 to 10^4 Rad²/s on a logarithmic scale, we plot the mean of correlation peak over this range, as well as the loss and variance of correlation peak as a function of σ_ϕ^2 .

The root mean square (RMS) and SNR of correlation peak can be calculated and plotted for every value of σ_ϕ^2 using Equations 34 and 35:

$$RMS = \sqrt{\mu_Y^2 + \sigma_Y^2} \quad (34)$$

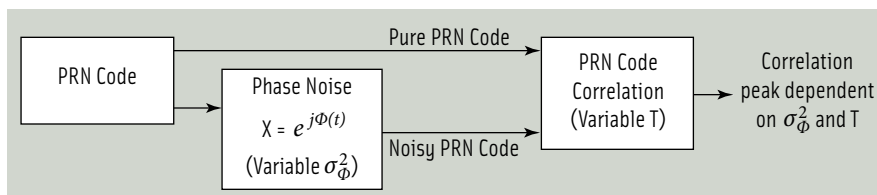


FIGURE 4 Numerical simulation for PRN code correlation

$$SNR = \frac{\sigma_Y^2}{\sigma_X^2} \quad (35)$$

The entire process can be repeated for different values of the PIT to show the combined effect of increasing phase noise and increasing T on the code correlation peak.

Correlation Model for Noisy and Noiseless PRN Codes

The numerical model presented earlier simulates a stand-alone correlation process between noisy and noiseless PRN codes. However, none of the real-world GNSS receiver blocks nor their effects on the code correlation process were simulated.

For the next step, we correlate noisy and noiseless PRN codes using a datastream model for a Galileo receiver. We simulate both the code and carrier tracking loops to show the effect of phase noise while using a closed-loop code correlation process.

A Galileo software signal generator, developed for research purposes at Tampere University of Technology, generates Galileo E1B/C signals as shown in **Figure 5**. For simplicity, navigation data bits are not included in the actual simulation. The PRN codes are modulated onto an intermediate frequency (IF) carrier signal of 3.42 MHz.

We model the communication channel as an ideal channel free from multipath, RF interference, or additive white Gaussian noise (AWGN). Noise contamination other than front-end oscillator phase noise is kept at a minimum by defining a high C/N_0 .

The datastream model for the Galileo E1 receiver is shown in **Figure 6**. The incoming signal from the communication channel is mixed with phase noise calculated in the same way as in the numerical model. Carrier wipe-off removes the IF signal, separates the inphase (I) and quadrature (Q) components and passes the combination of PRN code and phase noise to the code correlation block, where we correlate the signal with locally generated replicas of E1B/C PRN codes.

A single GPS correlator correlates over a pre-detection integration time of one millisecond while a single correlator for Galileo correlates over a pre-detection integration time of four milliseconds. Therefore, it is convenient to set pre-detection integration times for both the numerical and datastream models to multiples of four milliseconds. Equation 36 calculates the size of the signal vector in the datastream model:

$$L_{signal\ vector} = fs * 4\ ms \quad (36)$$

where f_s equals sampling frequency used in the datastream model. After the integration and dump (I&D) block, the I and Q components give the complex correlation output. Equation

37 is used to calculate the normalized magnitude of correlation peak:

$$C = \left(\frac{I}{L_{\text{signal vector}}}\right)^2 + \left(\frac{Q}{L_{\text{signal vector}}}\right)^2 \quad (37)$$

where, C equals magnitude of correlation, I equals In-phase component of correlation output, Q equals quadrature component of correlation output. If PIT is selected as the n th multiple of four milliseconds, the correlation output vector has n elements, and the total value of correlation peak is then a cumulative sum of all n values.

Similar to the numerical model, in the datastream model the phase noise variance σ_ϕ^2 is also varied from 0 to 10^4 Rad²/s on a logarithmic scale. Mean, loss, and variance of correlation peak are measured while RMS and SNR are calculated and plotted against σ_ϕ^2 . We carried out these simulations for PITs of 4, 8, 12, 20, and 100 milliseconds.

Results and Mathematical Interpretation

Figure 7 shows the plot for the loss of correlation peak versus phase noise variance per unit time (σ_ϕ^2) for various values of the PIT for the analytical (theoretical), numerical, and datastream models. Figures 8 and 9 show the variance and the RMS of the correlation peak versus σ_ϕ^2 .

Similarly, Figure 10 shows the SNR of correlation peak, while for simplicity only the results for intervals of 4, 12, and 100 milliseconds are plotted for the variance and SNR.

(A comparison between the theoretical model and the simulation models for variance of correlation peaks was already shown in Figure 3.) The results illustrate the validity of the simulation for a stand-alone, open-looped correlation process, even in a real-world receiver with fully functional carrier and code tracking loops.

Figure 7 indicates that the loss in correlation peak increases as phase noise increases. However, for larger T intervals, where for a particular σ_ϕ^2 the loss in correlation peak is larger. The maximum variance of correlation is approximately -13 decibels irrespective of T , but this

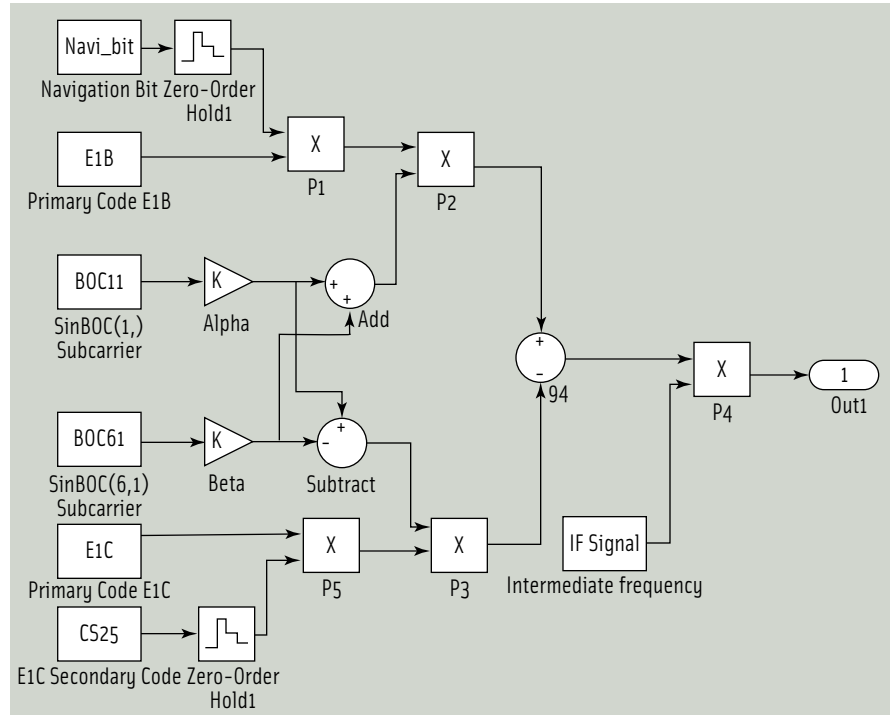


FIGURE 5 Galileo E1B/C signal generator shown schematically in datastream simulation

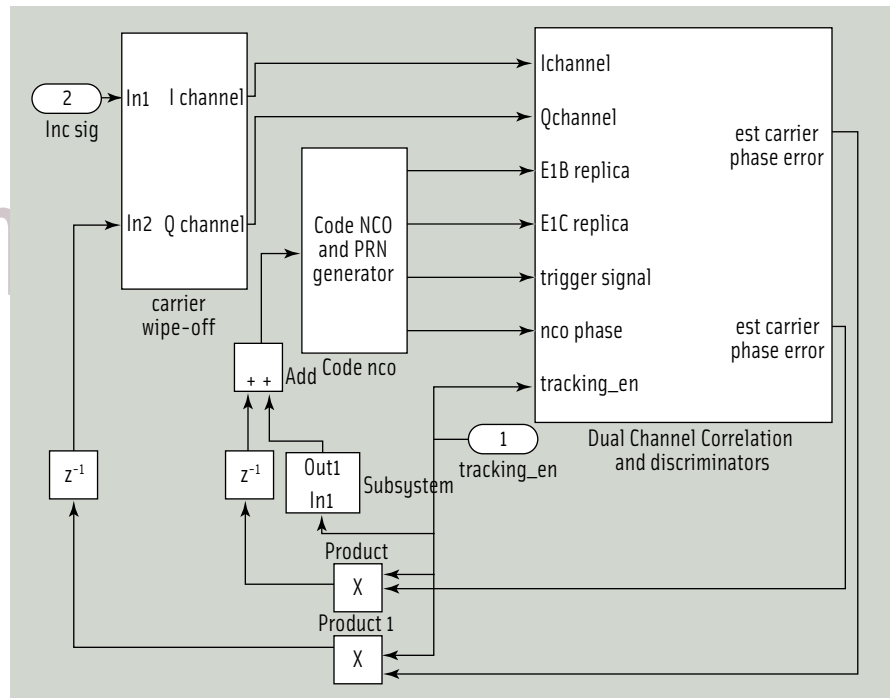


FIGURE 6 Galileo E1 receiver model

maximum is reached at lower values of σ_ϕ^2 with increasing T . This result is consistent with the explained interchangeability of T and σ_ϕ^2 in the expressions for this correlation degradation.

As PN_{variance} increases, the mean

and RMS of the correlation peak fall. The variance of the correlation peak increases up to a certain maximum and then also falls, but this decrease is in the region where the losses are already unsustainable. This result is

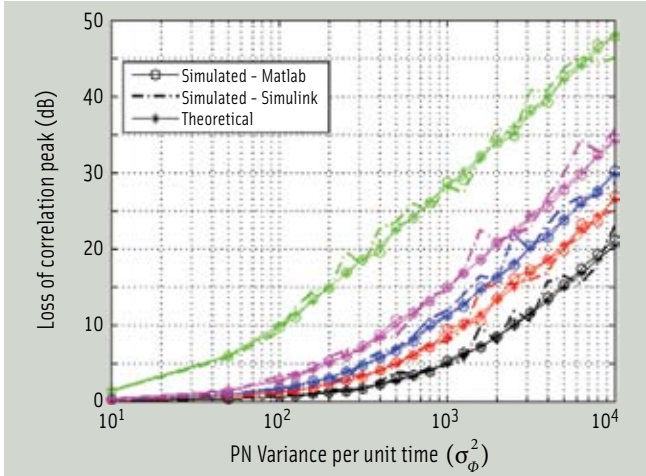


FIGURE 7 Loss of correlation peak versus phase noise variance (PIT: black = 4 milliseconds, red = 8 milliseconds, blue = 12 milliseconds, magenta = 20 milliseconds, green = 100 milliseconds).

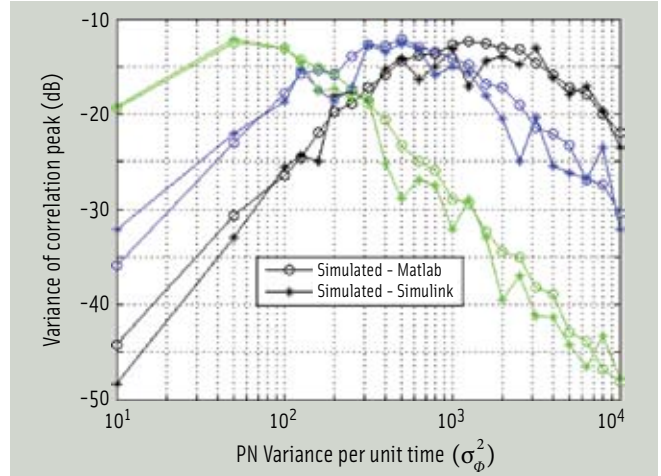


FIGURE 8 Variance of correlation peak versus phase noise variance (PIT: black=4 milliseconds, blue=12 milliseconds, green=100 milliseconds).

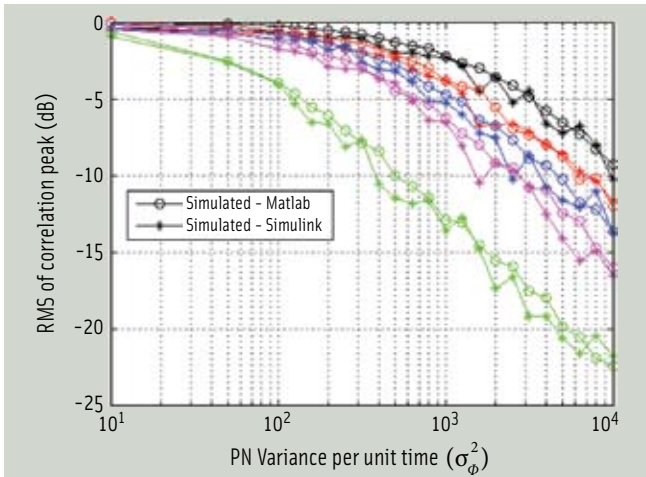


FIGURE 9 Figure 9 RMS of correlation peak versus phase noise variance (PIT: black = 4 milliseconds, red = 8 milliseconds, blue = 12 milliseconds, magenta = 20 milliseconds, green = 100 milliseconds)

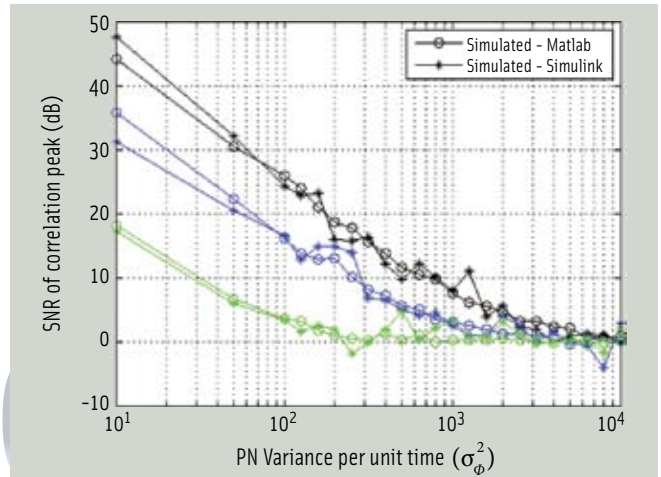


FIGURE 10 SNR of correlation peak versus σ_{ϕ}^2 (PIT: black = 4 milliseconds, blue = 12 milliseconds, green = 100 milliseconds)

reasonable, because the value of the correlation peak converges to zero.

Increasing the PIT above four milliseconds is also detrimental to the correlation output, because all the negative observations due to an increase in $PN_{variance}$ begin at lower values of σ_{ϕ}^2 . In other words, the maximum allowable input $PN_{variance}$ for a certain level of correlation peak RMS progressively decreases as we increase the PIT.

In the numerical and datastream simulations, an effective approach for identifying the maximum phase noise is to use a free-running local oscillator phase noise model, with a 10-decibel minimum correlation output SNR. Although these boundaries for the SNR criteria seem very stringent, we plan to use more realistic, practical models in which phase noise flattens below a given frequency offset. We expect that this condition will, in turn, modify the slope of the SNR so that the synthesizer requirements would become closer to the figures offered by real receivers.

In **Figure 10**, in order to maintain a minimum correlation SNR of 10 decibels when the PIT is 4 milliseconds, the maximum allowable σ_{ϕ}^2 is 251.2. For a PIT of 100 milliseconds, the maximum allowable σ_{ϕ}^2 to maintain a similar correlation SNR is 15.5. Using Equation 4, with a 4-millisecond PIT and frequency offset (f_m) of one megahertz, the maximum allowed phase noise is

$$PN_{max} = 10 \log_{10} \left(\frac{251.2}{(2\pi \cdot 1\text{MHz})^2} \right) = -112 \text{ dBc/Hz} \quad (38)$$

Similarly, for a PIT of 100 milliseconds, PN_{max} is -124 dBc/Hz, which means that, for longer integration intervals, phase noise requirements from front-end local oscillator become more stringent.

Figures 11 and **12** show the datastream simulation plots for the RMS and SNR of correlation peak in presence of multipath effects and additive white Gaussian noise (AWGN) channel imperfections. Two multipath components of half the power of

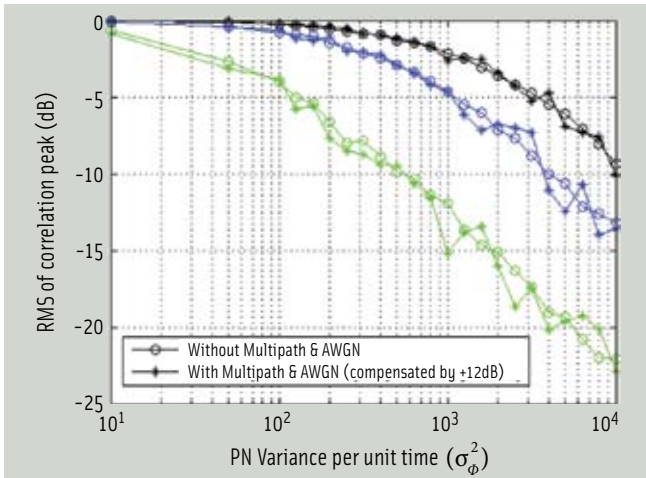


FIGURE 11 RMS of correlation peak in presence of multipath & AWGN (PIT: black = 4 milliseconds, blue = 12 milliseconds, green = 100 milliseconds)

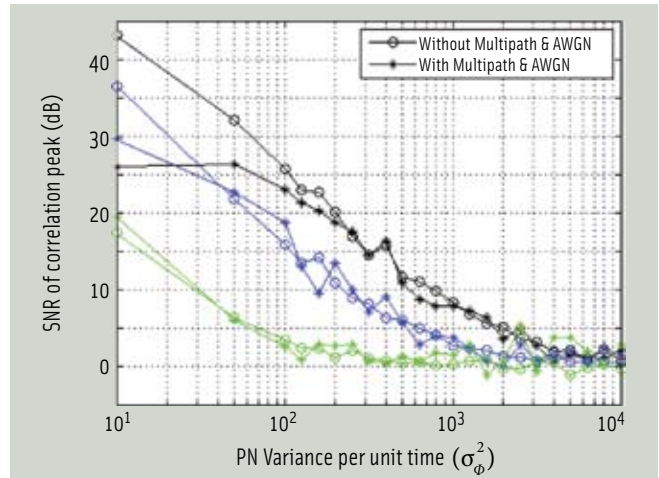


FIGURE 12 SNR of correlation peak in presence of multipath & AWGN (PIT: black = 4 milliseconds, blue = 12 milliseconds, green = 100 milliseconds)

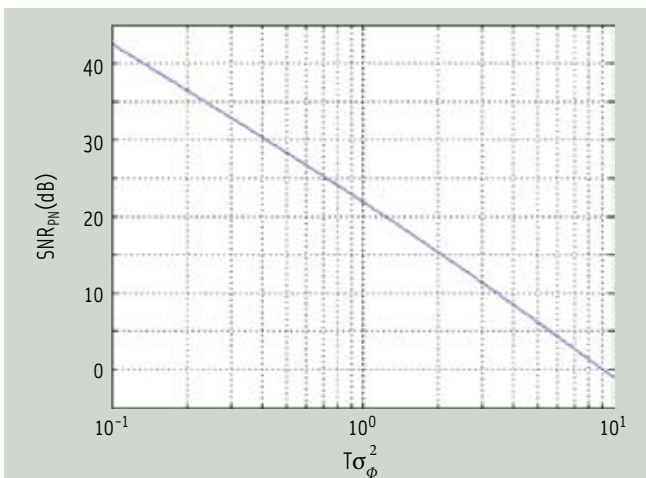


FIGURE 13 SNR_{PN} as a function of $T\sigma_{\phi}^2$

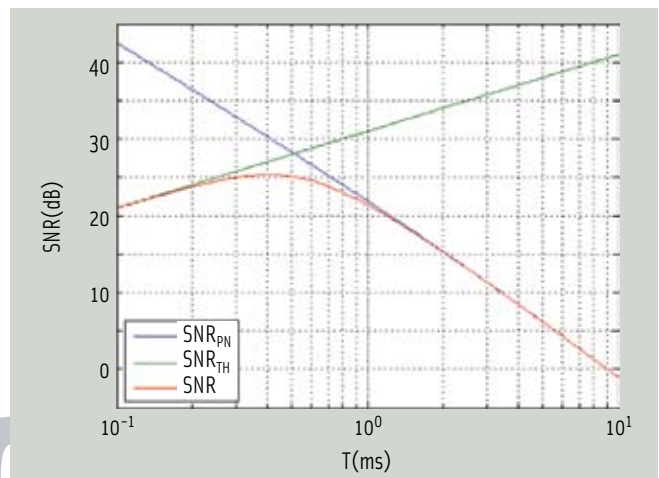


FIGURE 14 Thermal and phase noise contributions to SNR

the line of sight (LOS) component with delays of one chip and half chip, respectively, were added to the LOS component. AWGN was added such that overall carrier-to-noise ratio reduced by 25 decibels. For comparison, the numerical simulation results, absent the effects of multipath and AWGN, are also provided in the same figures.

Channel imperfections only result in a fixed attenuation of the overall RMS characteristics, in this case 12 decibels.

However, the shape of the curves and, hence, the effects of phase noise, remain unchanged. This can be easily demonstrated by compensating the datastream model curves with +12 decibels so that they match perfectly with the numerical model curves as shown in Figure 11.

In the case of SNR, the difference between curves with and without channel imperfections is higher for lower values of integration intervals and phase noise. This occurs because, as the integration interval, T , and PN increase, the SNR of correlation drops anyway, blunting the effect of channel imperfections.

to phase noise (SNR_{PN}), as a function of $T\sigma_{\phi}^2$ obtained after fitting with numerically computed data. For a given correlation time T , we can immediately obtain the maximum acceptable noise level σ_{ϕ} required to achieve a certain SNR or, conversely, the maximum acceptable integration interval T under a given noisy oscillator.

Regarding the latter, it is interesting to note that SNR due to thermal noise, SNR_{TH} , increases with integration time, while SNR due to phase noise under this model does exactly the opposite as shown in Figure 14. This limit is especially important in high-sensitivity receivers where integration periods are long, due to the quality of the local oscillator setting a boundary beyond which SNR can no longer be improved through coherent integration.

PIT (milliseconds)	Maximum Phase Noise (dBc/Hz)	
	$f_m=10$ (kilohertz)	$f_m=1$ (megahertz)
T = 4	-72	-112
T = 12	-74	-114
T = 100	-84	-124

TABLE 1. Maximum phase noise in order to maintain a minimum correlation SNR of 10 decibels for different values of PIT and f_m

Figure 13 represents the SNR due

Let us consider for example the case of GPS L1 C/A with a nominal SNR thermal or SNR_{TH} of 34 decibels for a T of 20 milliseconds, representing the worst case for phase noise. As thermal noise is minimal, the phase noise becomes a limiting factor sooner. If we set σ_{ϕ}^2 equals 100, the combined SNR is:

$$SNR = \left(\frac{1}{SNR_{TH}} + \frac{1}{SNR_{PN}} \right)^{-1} \quad (39)$$

Figure 14 clearly shows how the SNR increases with the correlation interval until the phase noise becomes dominant, under the assumption of negligible phase noise losses, compressing the SNR_{TH} curve. The optimal T in this case falls below 20 milliseconds, indicating non-coherent integration methods would be more appropriate under these assumptions.

Conclusion

This phase model is a conservative first approximation, illustrating the relationships between phase noise, thermal noise, and correlator performance. In this article, we first presented an analytical approach for evaluating the effects of the local oscillator phase noise in the performance of the correlators of a GNSS receiver. A mathematical model validated the analytical approach, and a datastream model demonstrated the tracking channel imperfections based on GNSS receiver implementations

We characterized the relationship between the integration time and phase noise, and presented a criterion for radio front-end design. We believe this model offers new tools for the analytical design of GNSS receivers, while laying a conservative boundary for their practical design.

Acknowledgments

The research leading to these results has received funding from the European Community Seventh Framework Program (FP7/2007-2013) under grant agreement number 227890. This work has also been supported by the Academy of Finland.

Manufacturers

The analytical portion of this study was

developed using Maple from **Maplesoft**, Waterloo, Ontario, Canada. The numerical model was developed using Matlab, and the datastream model utilized Simulink, both from **The Mathworks**, Natick, Massachusetts, USA.

Additional Resources

[1] Demir, A., "Phase Noise and Timing Jitter in Oscillators With Colored-Noise Sources," *IEEE Transactions on Circuits and Systems- Fundamental Theory and Application*, Vol. 49, No. 12, December 2002

[2] Demir, A., and A. Mehrotra and J. Roychowdhury, "Phase Noise in Oscillators: a Unifying Theory and Numerical Methods for Characterization," *IEEE Transactions on Circuits and Systems I: Fundamental Theory and Applications*, Vol. 47, No 5, May 2000, pp. 655-674, DOI 10.1109/81.847872

[3] Hajimiri, A., and T. H. Lee, "A general theory of phase noise in electrical oscillators", *IEEE J. Solid-State Circuits*, vol. 33, pp. 179-194, February 1998

[4] Irsigler, M., and B. Eissfeller, "PLL Tracking Performance in the Presence of Oscillator Phase Noise," *GPS Solutions*, Volume 5(4), pp. 45-57, Spring 2002

[5] Kundert, K., "Predicting the Phase Noise and Jitter of PLL-Based Frequency Synthesizers," *The Designer's Guide Community* <www-designers-guide.org>, Designer's Guide Consulting Inc., August 2006

[6] Leeson, D.B., "Simple model of feedback oscillator noise spectrum," *Proceedings IEEE*, p.369, February 1966

[7] Petovello, M., and E. Falletti, M. Pini, and L. Presti, "Are Carrier-to-Noise Algorithms Equivalent in All Situations?" *GNSS Solutions*, *Inside GNSS*, pp. 20-27, January/February 2010

[8] Petrovic, D., and W. Rave and G. Fettweis, "Effects of Phase Noise on OFDM Systems With and Without PLL: Characterization and Compensation," *IEEE Transactions on Communications*, Vol. 55, No. 8, Aug 2007

[9] Rebeyrol, E., and C. Macabiau, L. Ries, J-L. Issler, M. Bousquet, and M-L. Boucheret, "Phase Noise in GNSS Transmission/Reception System," *Proceedings of the 2006 National Technical Meeting of the Institute of Navigation*, January 18-20, 2006, Monterey, California, USA

[10] Sauvage, G., "Phase Noise in Oscillators: A Mathematical Analysis of Leeson's Model," *IEEE Transactions on Instrumentation and Measurement*, Vol. IM-26, No. 4, December 1977

[11] Schenk, T., "Phase Noise," Chapter 4 of *RF Imperfections in High-rate Wireless Systems*, ISBN: 978-1-4020-6902-4, Springer 2008

[12] Schenk, T. (2006), "RF Impairments in Multiple Antenna OFDM - Influence and Mitigation," Ph.D. Thesis, Technical University of Eindhoven, November 2006

[13] Syrjälä, V. and M. Valkama, "Analysis and mitigation of phase noise and sampling jitter in OFDM radio receivers," *European Microwave Association, International Journal of Microwave and Wireless Technologies*, vol. 2, pp. 193-202, April 2010

[14] Syrjälä, V., and M. Valkama, N. N. Tchamov, and J. Rinne, "Phase Noise Modelling and Mitigation Techniques in OFDM Communication Systems," *Wireless Telecommunication Symposium*, WTS 2009, April 2009, pp.1-7

Authors



Ernesto Pérez Serna obtained his M.Sc. degree in telecommunications engineering at the University of Cantabria (Spain), where he later worked within the

Department of Communications Engineering (DICOM) from 2005 to 2006, designing SiGe and Si CMOS PLL frequency synthesizers for RF receivers. He joined ACORDE in 2006 as R&D engineer, mainly designing custom CMOS RF and digital ICs for GNSS applications. He has been involved in all the ASIC designs of the FP6 GREAT project and the MAGNET BEYOND transmitter and has published several papers in the area of MMIC design. He is currently working towards his master's degree in information technology and mobile communications and a Ph.D. in telecommunications at the University of Cantabria.



Sarang Thombre received his B.Sc. degree (with Distinction) in electronics and telecommunications engineering (E&TC) from University of Pune (UoP), India and his

M.Sc. degree (with Distinction) from Tampere University of Technology (TUT), Finland in radio frequency electronics. Currently, he is working as a researcher and Ph.D. student with the Department of Computer Systems at TUT, Finland. His general research interests are in software based simulation of GNSS signals and design and analysis of radio front-ends for GNSS receivers.



Mikko Valkama received the M.Sc. and Ph.D. degrees (both with honors) in electrical engineering (EE) from Tampere University of Technology (TUT), Finland. In 2002 he received the "Best Ph.D. Thesis"

award from the Finnish Academy of Science and Letters for his dissertation entitled "Advanced I/Q signal processing for wideband receivers: Models and algorithms." Currently, he is a full professor in the Department of Communications Engineering at TUT. His general research interests include communications signal processing, estimation and detection techniques, signal processing algorithms for software defined and cognitive radios, different sampling methods including compressive sampling, digital transmission techniques such as different variants of multicarrier modulation methods and OFDM, and radio resource management for ad-hoc and mobile networks.



Simona Lohan has been an adjunct professor in the Department of Communications Engineering, Tampere University of Technology since 2007. She obtained her Ph.D.

degree in wireless communications from Tampere University of Technology and also graduated with an M.Sc. in electrical engineering from "Politehnica" University of Bucharest, Romania, and with a D.E.A. (French equivalent of master's degree) in econometrics from Ecole Polytechnique, Paris, France. Lohan is currently leading the research activities in signal processing for wireless communications in the Department of Communications Engineering, TUT. She is the principal investigator in a research project funded by the Academy of Finland focusing on indoor location and has been involved as technical group leader in two European GNSS-related projects, within FP6 and FP7: "GREAT" and "GRAMMAR," dealing with Galileo mass-market receivers.



Ville Syrjälä received the M.Sc. degree (with honors) in communications engineering (CS/EE) from Tampere University of Technology (TUT), Finland. Currently, he is

working as a researcher with the Department of Communications Engineering at TUT, Finland. His general research interests are in communications signal processing and signal processing algorithms for flexible radios.



Marco Detratti received the Laurea degree (M.Sc.) in electronic engineering from the University of Perugia (Italy) and the DEA (Diploma of Advanced Studies) from the University of Cantabria (Spain). He joined

ACORDE in 2005 to develop custom RF solutions for satellite applications. At present he is leading

the GNSS department and is in charge of the development of navigation products and RF equipment within the company portfolio. Detratti has been the "responsible" of the ASIC front-end developments within FP6 GREAT Project and of the platform of the FP6 MAGNET/BEYOND project. At present he is acting as technical manager of the FP7 GRAMMAR project for the development of an advanced multi-frequency GNSS receiver.




Heikki Hurskainen received an M.Sc. degree in electrical engineering and doctoral degree in computing and electrical engineering from Tampere University of Technology (TUT), Finland. Currently, Hurskainen is

working as a research fellow at TUT's Department of Computer Systems, where he continues to work in satellite navigation research projects. His research interests include, but are not restricted to, evolution of GNSSes, implementation and prototyping issues of receiver algorithms, and emerging applications of GNSS receivers.



Jari Nurmi is a professor of computer systems at Tampere University of Technology (TUT), where obtained a Ph.D. degree and currently leads a group of about 20

researchers. He has held various research, education and management positions at TUT and in the industry since 1987. His current research interests include system-on-chip integration; embedded and application-specific processor, multiprocessor and reconfigurable architectures; and circuit implementations of positioning, DSP, and digital communication systems (including software-defined radio approach). Nurmi is the general chairman of the annual International Symposium on System-on-Chip (SoC) and its predecessor SoC Seminar in Tampere since 1999 and is now editing Springer books on *Galileo Positioning Technology* and *Computation Platforms for SDR*. In 2004, he was one of the recipients of Nokia Educational Award, and the recipient of Tampere Congress Award 2005. 



browse the
digital
edition

insidegnss.com